Electronic Supplementary Information

Boosting ultralong organic phosphorescence performance by synergistic heavy-atom effect and multiple intermolecular interactions in molecular crystal

Huiting Mao,[‡ a,b,c] Jing Gao, [‡a] Weijun Zhao,[d] Tingting Wang,[a] Guo-Gang Shan,[a,*] Yun Geng,[a,*] Kuizhan Shao,[a] Xinlong Wang[a] and Zhongmin Su[c*]

[a]*Institute of Functional Material Chemistry and National & Local United Engineering Lab for Power Battery, Faculty of Chemistry, Northeast Normal University, Changchun, 130024, China, E-mail: shangg187@nenu.edu.cn (G. S.), gengy575@nenu.edu.cn (Y. G.)*

[b]*College of Life Science, Dalian Minzu University, Dalian, 116600, China*

[c]*College of Chemistry, Jilin University, Changchun, Jilin, 130012, China*

E-mail: zmsu@nenu.edu.cn

[d]*School of Chemistry and Molecular Engineering, East China University of Science & Technology, Shanghai, 200237, China*

[‡]*Authors contributed equally to this paper.*

Experimental section

Materials and methods

Unless otherwise noted, all reagents used in the experiments were purchased from commercial sources without further purification. For column chromatography, silica gel with 300~400 mesh was used. These compounds were synthesized according to the similar experimental procedures reported previously. Nuclear magnetic resonance (^{1}H and ^{13}C NMR) spectra were obtained on a Bruker Avance 500 MHz spectrometer. High-resolution mass spectra (HRMS) were tested on Bruck microtof or Hybrid Quadrupole-Orbitrap GC-MS/MS system (Q Exactive GC). X-ray crystallography was measured by a Bruker Apex CCD II area-detector diffractometer. Ultraviolet absorption spectra were obtained by Cary 500 UV-Vis-NIR spectrophotometer. Steady-state photoluminescence (PL) and phosphorescence spectra were measured using FL-4600 FL spectrophotometer. The lifetime and time-resolved emission spectra were obtained on FLSP920 Edinburgh Fluorescence Spectrometer equipped with a xenon arc lamp (Xe900), a nanosecond hydrogen flash-lamp (nF920), and a microsecond flash-lamp (μF900), respectively. PL quantum efficiency (PLQE) was collected on a Hamamatsu Absolute PL Quantum Yield Spectrometer C11347 under ambient conditions.

Theoretical calculations

The geometrical, electronic structures and relevant photophysical properties are calculated with the Gaussian 16,[1] ADF 2016[2] and MOMAP[3] program packages. The density functional theory (DFT) and time-dependent density functional theory (TDDFT)[4] are selected for calculated molecules in ground states and excited states, respectively. The geometrical structures of monomers and dimers taken from the experimental crystals are optimized at B3LYP/6-311G* and B3LYP-D3/6-311G* level, respectively. The excitation energies and oscillator strengths are also calculated at the same computational level. Considering the intermolecular interaction effects, the Quantum Mechanics/Molecular Mechanics (QM/MM) method[5] is used to optimize the geometrical structures of the dimers.

The chosen dimers are calculated at the QM level and the surrounding molecules are treated at MM level with the universal force field (UFF).[6] The spin-orbital coupling (SOC) matrix element values are calculated by the ADF 2016 program package with the B3LYP functional and the ZORA/DZP basis set.[7]

The reorganization energy (λ) can be calculated by Nelson's four-point method:

$$\lambda_{T_1} = \lambda_1(H) + \lambda_2(G) = \left[E\left({}^3H_{fc}\right) - E\left({}^3H_{opt}\right)\right] + \left[E\left({}^0G_{fc}\right) - E\left({}^0G_{opt}\right)\right] \quad (1)$$

$$\lambda_{S_0} = \lambda_1(H) + \lambda_2(G) = \left[E\left({}^1H_{fc}\right) - E\left({}^1H_{opt}\right)\right] + \left[E\left({}^0G_{fc}\right) - E\left({}^0G_{opt}\right)\right] \quad (2)$$

where opt and fc represent the optimized states and Franck-Condon excited states, respectively. The spin multiplicity is labeled as the superscript.

The MOMAP software is used to calculate the Huang-Rhys factor:

$$HR_j = \omega_j D_j^2/2\hbar \quad (3)$$

Where ω_j represents the frequency of a certain vibration mode, D_j represents the displacement vector in a certain vibration mode.

Single crystal cultivation

All the crystals were obtained via slow evaporation in a mixture of dichlromethane/ethyl acetate (3:1, v/v) at room temperature.

The preparation of encryption and anti-counterfeiting patterns

The ink based on ***o*-MOPP** and **BrTMOPP** powder was firstly prepared with aloe vera gel. Then the ink was printed onto a piece of black paper with screen printing technique. After heat treatment for 30 minutes, a pattern with UOP feature was obtained. The lotus, lantern, and "Fu" (made by **BrTMOPP**) and auspicious cloud (made by ***o*-MOPP**) were clearly visualized under 365 nm UV-lamp irradiation. When switching off the UV-lamp, only lotus, lantern, and "Fu" with green emission can be observed by the naked eye. The preparation method of double crane pattern was described above.

Synthesis and characterization

Synthesis of 10-(4-bromo-3-methylphenyl)-10*H*-phenothiazine 5,5-dioxide (BrMOPP). Into a round-bottom flask was placed toluene solution (100 mL) with phenothiazine (2.00 g, 10 mmol), 1-bromo-4-iodo-2-methylbenzene (3.58 g, 12 mol), potassium tert-butoxide (1.69 g, 15 mmol), palladium acetate (0.11 g, 0.5 mmol), and tri-tert-butylphosphine (0.5 mL, 0.25 mmol). Then the mixture was stirred at 110 °C for 12 hours. The reaction mixture was extracted with CH_2Cl_2 for three times. Then the organic layer was collected and dried with Na_2SO_4. The solvent was removed by rotary evaporation, and the residue was purified by column chromatography. Then the collected product was added to CH_2Cl_2 (90 mL), acetic acid (45 mL), and H_2O_2 (2 mL). After stirring for 24 hours at 60 °C, the mixture was extracted with CH_2Cl_2 and further purified by column chromatography, affording a white solid in a yield of 81%. ^{1}H NMR (500 MHz, $CDCl_3$, δ [ppm]): 8.16 (dd, J = 8.0, 1.5 Hz, 2H, Ar H), 7.86 (d, J = 8.0 Hz, 1H, Ar H), 7.39-7.42 (m, 2H, Ar H), 7.24-7.27 (m, 3H, Ar H), 7.10 (dd, J = 8.5, 2.5 Hz, 1H, Ar H), 6.65 (d, J = 8.5 Hz, 2H, Ar H), 2.50 (s, 3H; CH_3). ^{13}C NMR (125 MHz, $CDCl_3$, δ [ppm]): 141.88, 140.53, 137.92, 135.14, 132.86, 132.56, 129.32, 126.30, 123.47, 122.76, 122.24, 117.14, 23.19. MS [m/z]: Calcd for $C_{19}H_{14}BrNO_2S$: 398.9929, Found 421.9813 $[M + Na]^+$.

Synthesis of 10-(4-bromo-3,5-dimethylphenyl)-10*H*-phenothiazine 5,5-dioxide (BrDMOPP). Following the similar procedure to **BrMOPP**, just changing the 1-bromo-4-iodo-2-methylbenzene to 2-bromo-5-iodo-1,3-dimethylbenzene. A white solid was obtained in the yield of 78%. ^{1}H NMR (500 MHz, $CDCl_3$, δ [ppm]): 8.16 (dd, J = 8.0, 1.5 Hz, 2H, Ar H), 7.39-7.42 (m, 2H, Ar H), 7.24-7.27 (m, 2H, Ar H), 7.11 (s, 2H, Ar H), 6.68 (d, J = 8.5 Hz, 2H, Ar H), 2.52 (s, 6H; CH_3). ^{13}C NMR (125 MHz, $CDCl_3$, δ [ppm]): 141.92, 140.52, 137.14, 132.78, 129.63, 128.83, 123.37, 122.63, 122.10, 117.22, 24.09. MS [m/z]: Calcd for $C_{20}H_{16}BrNO_2S$: 413.0085, Found 435.9983 $[M + Na]^+$.

Synthesis of 10-(4-bromo-2,3,5,6-tetramethylphenyl)-10*H*-phenothiazine 5,5-dioxide (BrTMOPP). Phenothiazine (2.00 g, 10 mmol), 1,4-dibromo-2,3,5,6-tetramethylbenzene

(3.52 g, 12 mol), sodium tert-butoxide (1.44 g, 15 mmol), bis(dibenzylideneacetone)palladium (1.16 g, 2 mmol), and tri-tert-butylphosphine (0.5 mL, 0.25 mmol) were added in toluene (100 mL). Then the mixture was stirred at 110 °C for 12 hours. And then, The mixture was extracted with CH_2Cl_2. The solvent was evaporated by rotary evaporation under vacuum and the product was purified by column chromatography. Then the collected product was added to CH_2Cl_2 (90 mL), acetic acid (45 mL), and H_2O_2 (2 mL). After stirring for 24 hours at 60 °C, the mixture was extracted with CH_2Cl_2 and further purified by column chromatography, affording a white solid in a yield of 61%. ^{1}H NMR (600 MHz, $CDCl_3$, δ [ppm]): 8.20 (dd, J = 7.8, 1.8 Hz, 2H, Ar H), 8.40-7.43 (m, 2H, Ar H), 7.25-7.28 (m, 2H, Ar H), 6.49 (d, J = 9.0 Hz, 2H, Ar H), 2.53 (s, 6H; CH_3), 1.95 (s, 6H; CH_3). ^{13}C NMR (150 MHz, $CDCl_3$, δ [ppm]): 138.86, 136.94, 134.85, 133.34, 130.57, 123.67, 122.71, 122.26, 116.17, 21.44, 15.68. MS [m/z]: Calcd for $C_{22}H_{20}BrNO_2S$: 441.0398, Found 464.0291 $[M + Na]^+$.

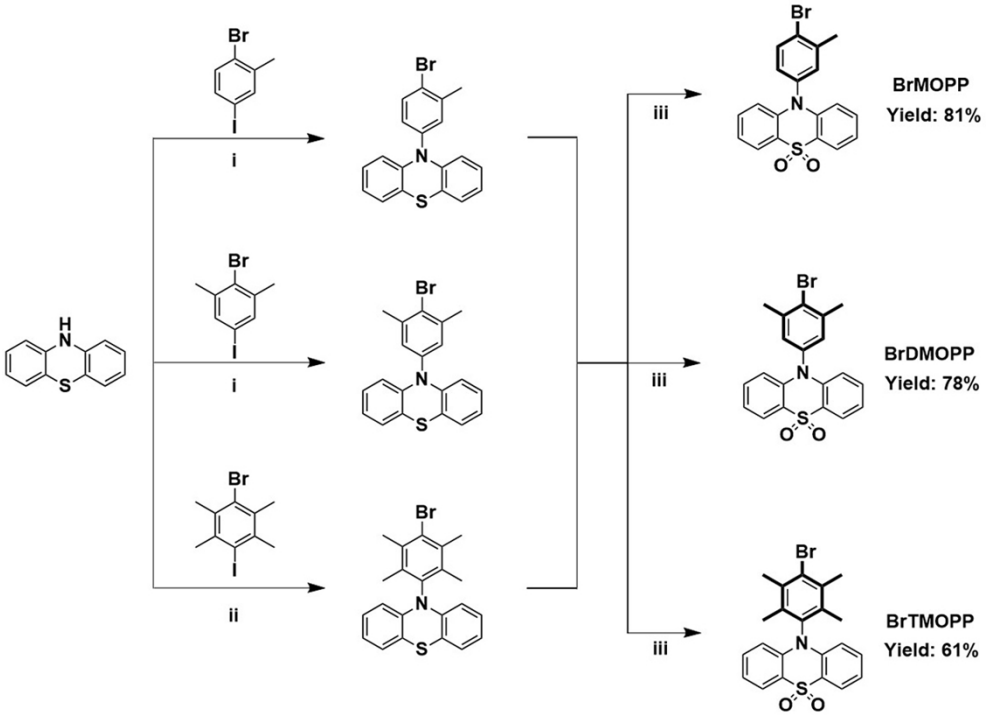

Scheme S1. Synthetic routes and chemical structures of **BrMOPP**, **BrDMOPP**, and **BrTMOPP**. (i) *t*-BuOK, $Pd(OAc)_2$, P(*t*-Bu)$_3$, Toluene, 110 °C. (ii) *t*-BuONa, $Pd(dba)_2$, P(*t*-Bu)$_3$, Toluene, 110 °C. (iii) H_2O_2, CH_2Cl_2/CH_3COOH, 60 °C.

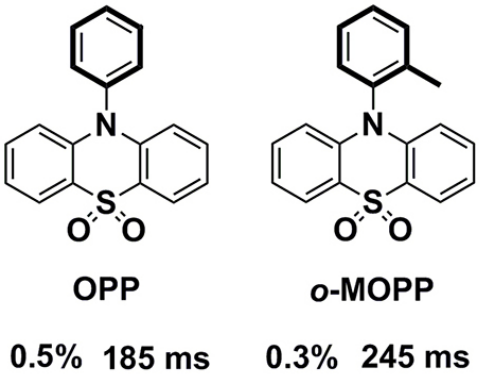

Scheme S2. Chemical structures of **OPP** and ***o*-MOPP**.

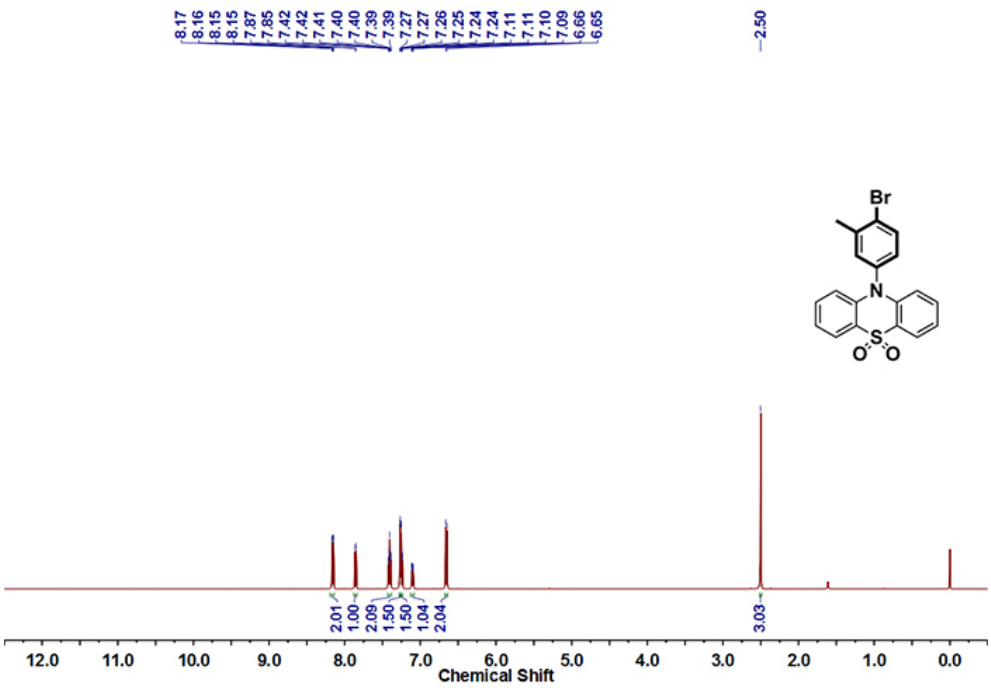

Fig. S1 ^{1}H NMR of **BrMOPP** in $CDCl_3$.

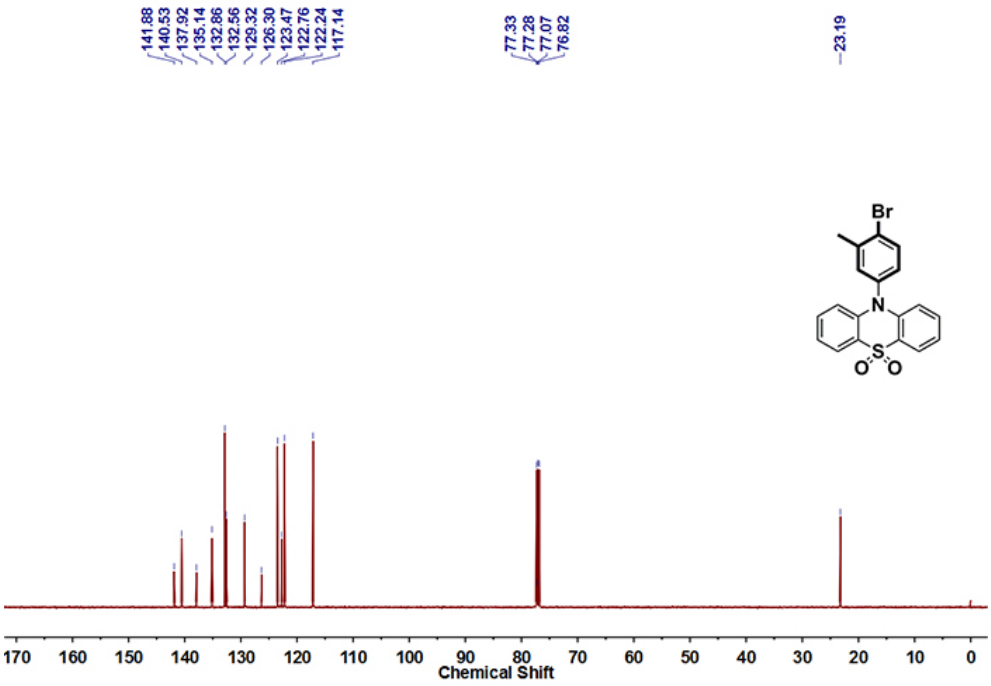

Fig. S2 ^{13}C NMR of **BrMOPP** in $CDCl_3$.

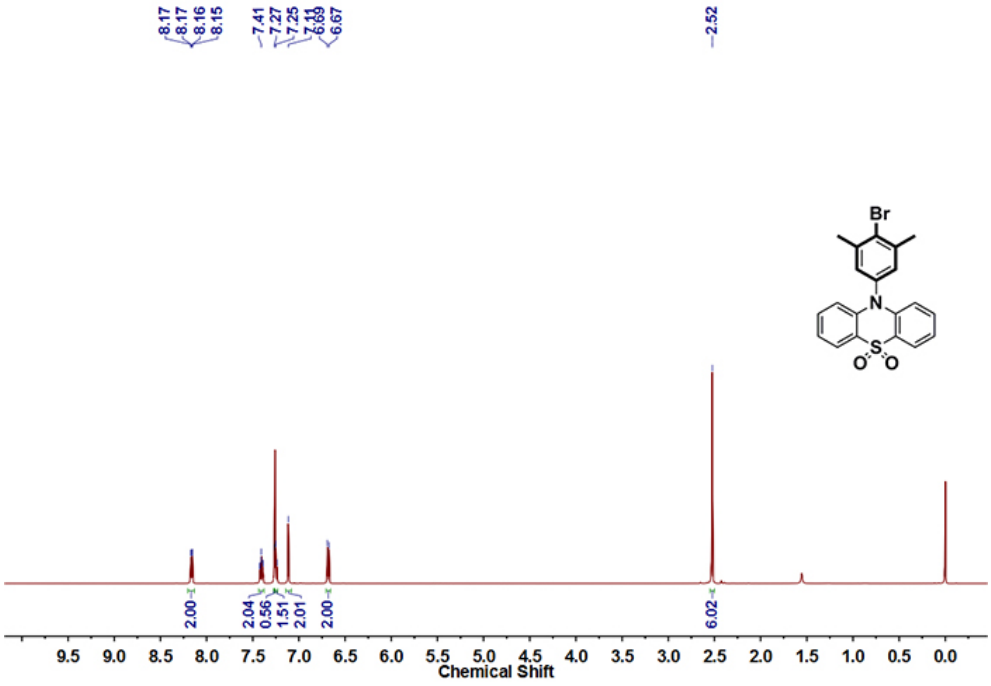

Fig. S3 ^{1}H NMR of **BrDMOPP** in $CDCl_3$.

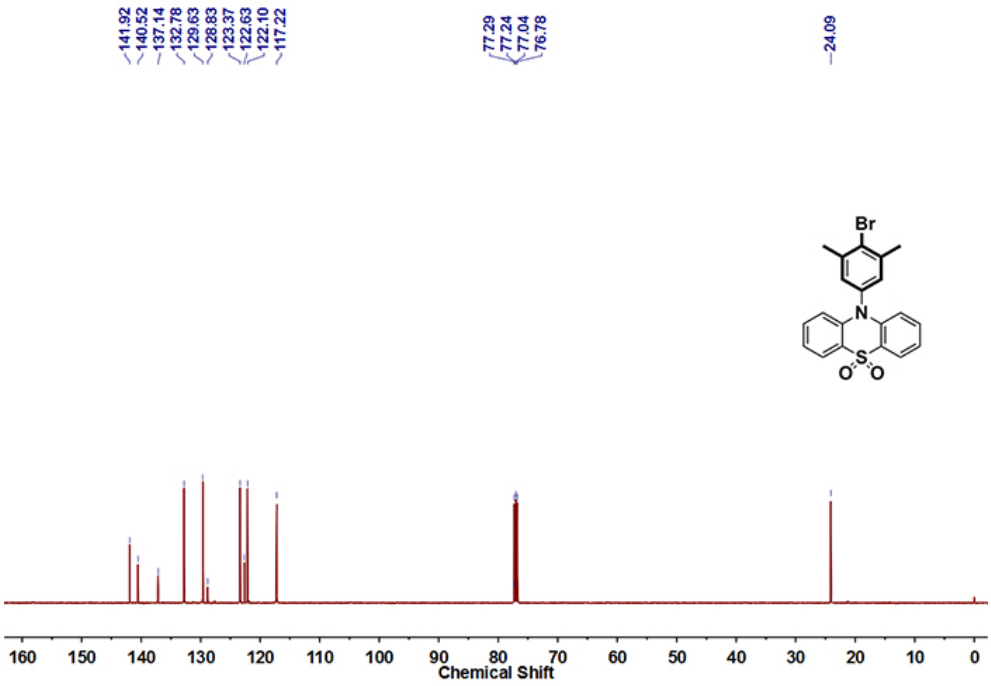

Fig. S4 ^{13}C NMR of **BrDMOPP** in $CDCl_3$.

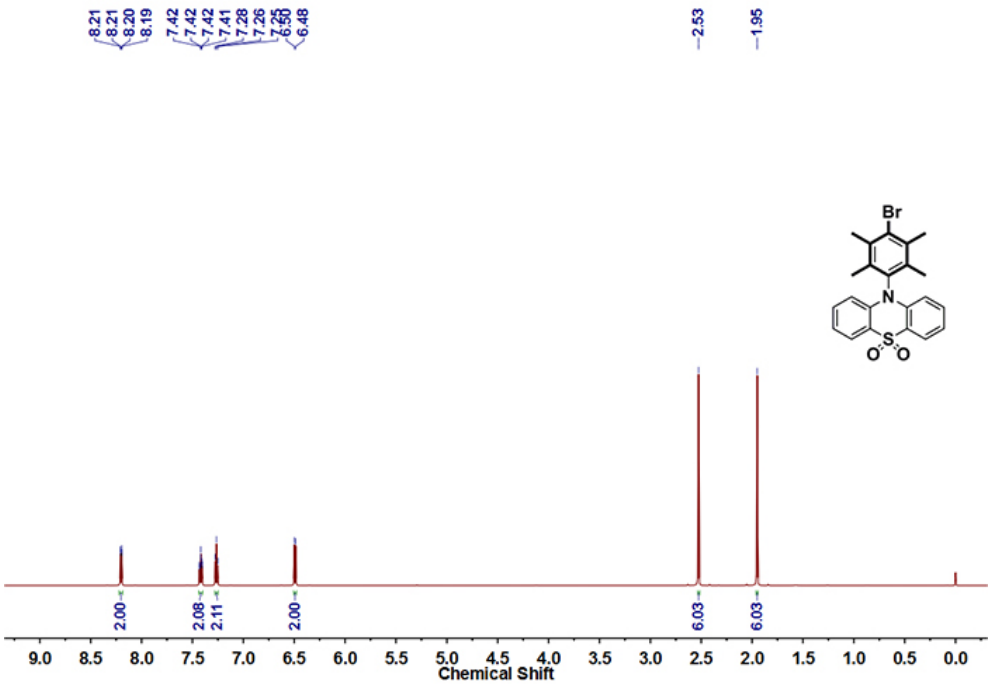

Fig. S5 ^{1}H NMR of **BrTMOPP** in $CDCl_3$.

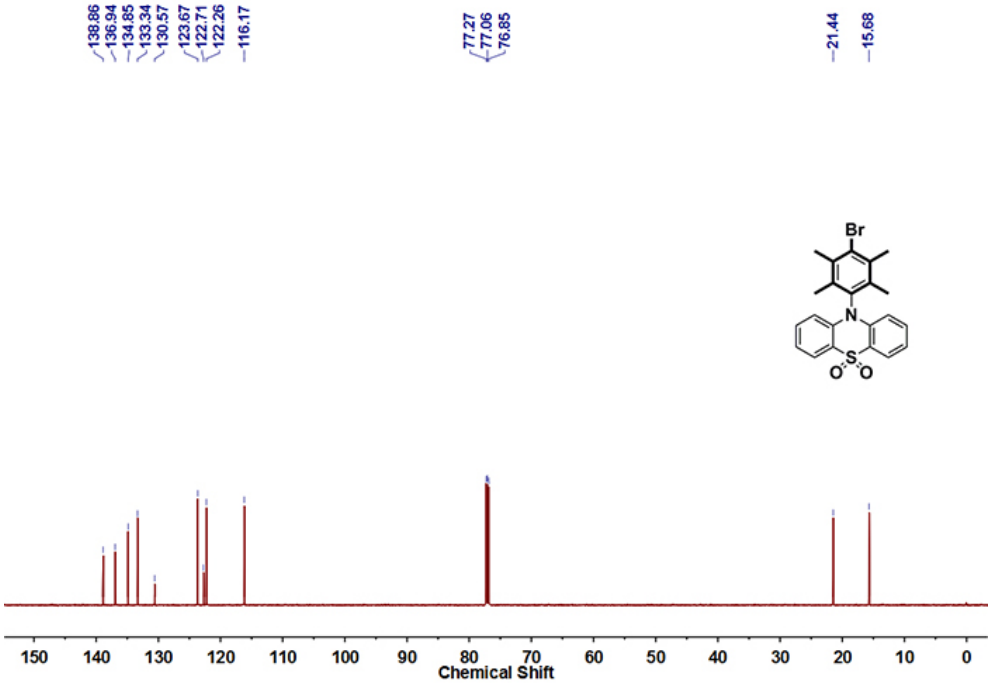

Fig. S6 ^{13}C NMR of **BrTMOPP** in $CDCl_3$.

Table S1. Crystal data and structure refinement of these compounds.

Name	**BrMOPP**	**BrDMOPP**	**BrTMOPP**
CCDC	2042977	2042978	2042979
Formula	$C_{19}H_{14}BrNO_2S$	$C_{20}H_{16}BrNO_2S$	$C_{22}H_{20}BrNO_2S$
Formula weight	400.28	414.31	442.36
Crystal system	triclinic	triclinic	triclinic
Space group	P-1	P-1	P-1
Cell Lengths (Å)	a 8.126(2) b 8.146(2) c 13.660(4)	a 8.2210(16) b 8.4240(17) c 14.349(3)	a 8.3574(8) b 9.3223(11) c 14.2727(16)
Cell Angles (°)	α 95.851(15) β 97.291(16) γ 112.652(14)	α 94.358(15) β 98.812(13) γ 114.597(13)	α 73.231(7) β 83.188(6) γ 64.864(5)
Cell Volume (Å^3)	816.4(4)	882.0(3)	963.87(19)
Z	2	2	2
$D_{calcd.}$(g m^{-3})	1.628	1.560	1.524
F(000)	404.0	420.0	452.0
R_{int}	0.0664	0.0939	0.0747
F^2	1.038	1.039	1.074

R_1[a], wR_2[b]	0.0804, 0.2703	0.0809, 0.2200	0.0446, 0.0971
R_1, wR_2	0.0890, 0.2865	0.1142, 0.2506	0.0658, 0.1090

[a] $R_1 = \Sigma||F_o|-|F_c||/\Sigma|F_o|$. [b] $wR_2 = |\Sigma w(|F_o|^2-|F_c|^2)|/\Sigma|w(F_o^2)^2|^{1/2}$.

Table S2. The intermolecular interactions of **BrMOPP**, **BrDMOPP**, and **BrTMOPP** crystals.

BrMOPP		**BrDMOPP**		**BrTMOPP**	
Types of bond	distance (Å)	Types of bond	distance (Å)	Types of bond	distance (Å)
π…π	3.387	π…π	3.458	π…π	3.496
C-H…Br	3.035	C-H…Br	2.855	C-H…Br	2.964
C-H…π	2.864	-	-	C-H…π	2.875
				C-H…H-C	2.378
	2.472		2.496		2.446
C-H…O	2.561	C-H…O	2.568	C-H…O	2.470
	2.625		2.690		2.705
S=O…C	3.129	S=O…C	3.156	S=O…C	3.218

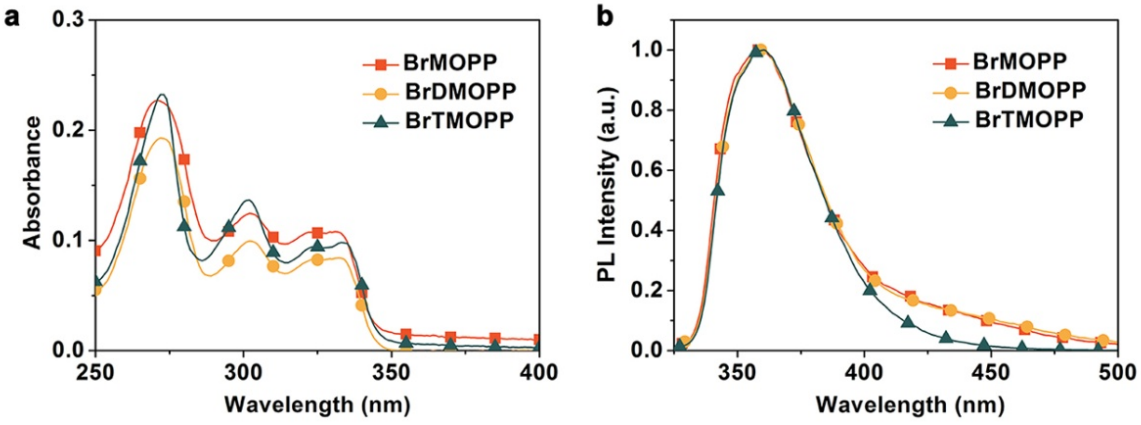

Fig. S7 (a) Absorption spectra and (b) steady-state PL spectra of **BrMOPP**, **BrDMOPP**, and **BrTMOPP** in dilute dichloromethane solutions (10^{-5} M) under ambient conditions.

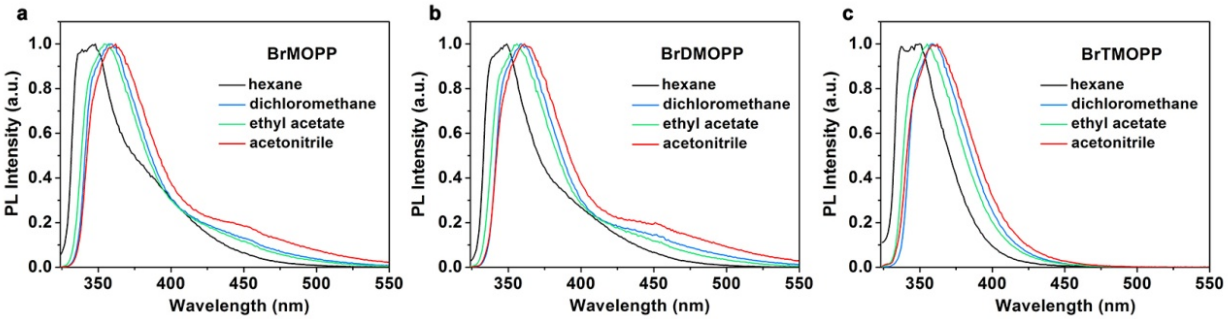

Fig. S8 PL spectra of **BrMOPP**, **BrDMOPP**, and **BrTMOPP** in different solvents (hexane, dichloromethane, ethyl acetate, and acetonitrile) with concentration of 5×10^{-5} M.

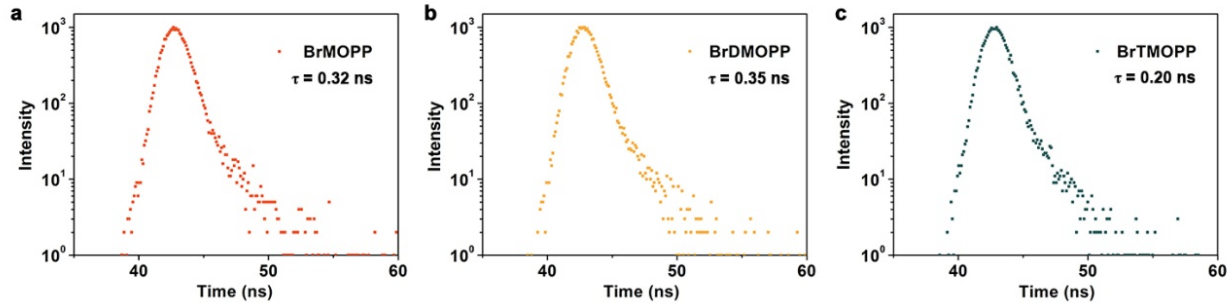

Fig. S9 Time-resolved PL decay curves of (a) **BrMOPP** at 359 nm, (b) **BrDMOPP** at 359 nm, (c) **BrTMOPP** at 360 nm in dichloromethane solutions under ambient conditions.

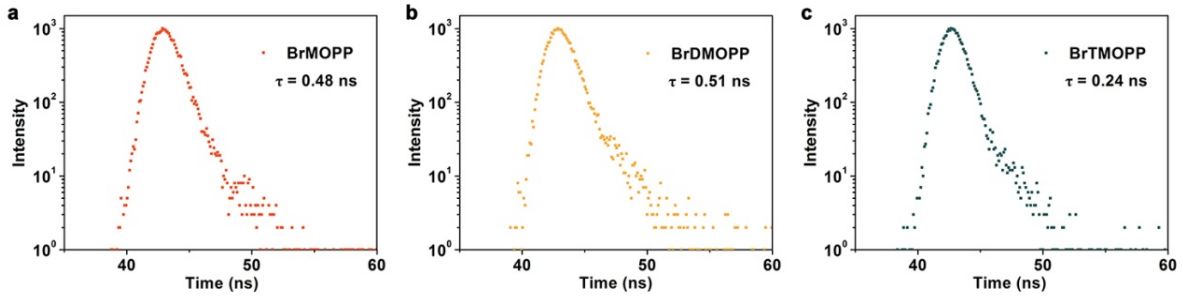

Fig. S10 Time-resolved PL decay curves of (a) **BrMOPP** at 375 nm, (b) **BrDMOPP** at 375 nm, (c) **BrTMOPP** at 368 nm in crystal state under ambient conditions.

Table S3. Summarized photophysical data of **BrMOPP**, **BrDMOPP**, and **BrTMOPP** in crystal state at 298 K.

Compound	λ_F (nm)	τ_F (ns)	Φ_F (%)	λ_P (nm)	τ_P (ms)	Φ_P (%)	k_{isc} (s^{-1})	k_r (s^{-1})	k_{nr} (s^{-1})
BrMOPP	375	0.48	4.8	512	391	11.1	2.3×10^8	0.28	2.27
BrDMOPP	375	0.51	3.6	500	255	8.4	1.6×10^8	0.33	3.59
BrTMOPP	368	0.24	1.6	519	664	4.0	1.7×10^8	0.06	1.44

λ_F: fluorescent emission peak; τ_F: fluorescent lifetime; λ_P: phosphorescent emission peak; τ_F: phosphorescent lifetime; Φ_P: quantum yield.

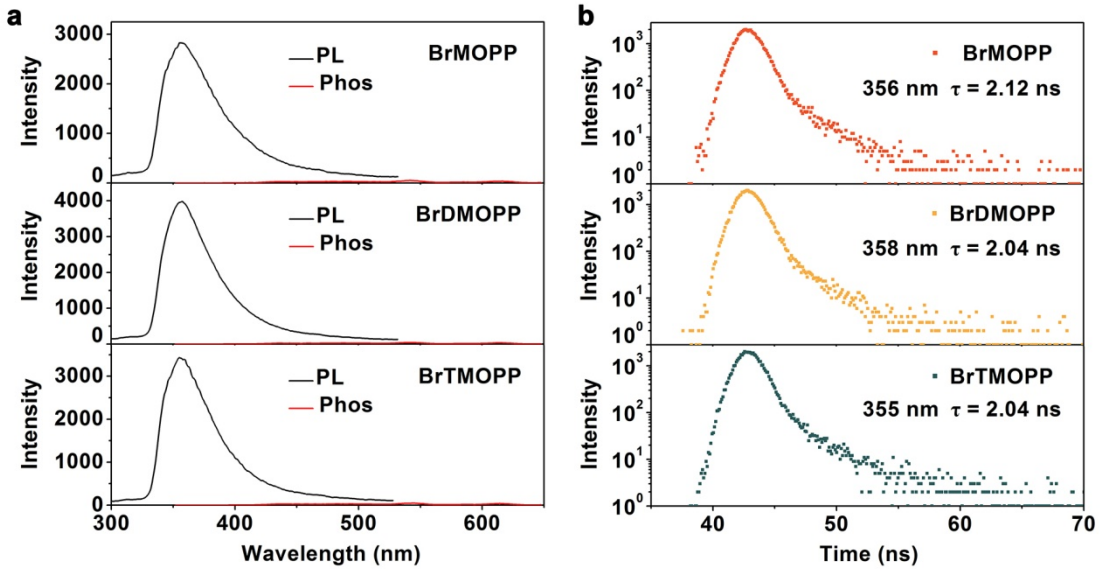

Fig. S11 (a) Steady-state photoluminescence (PL) (black line) and phosphorescence (Phos) spectra (red line) and (b) the time-resolved fluorescence decay curves of **BrMOPP**, **BrDMOPP**, and **BrTMOPP** doped in PMMA films (5 wt%) under ambient conditions excited at 330 nm.

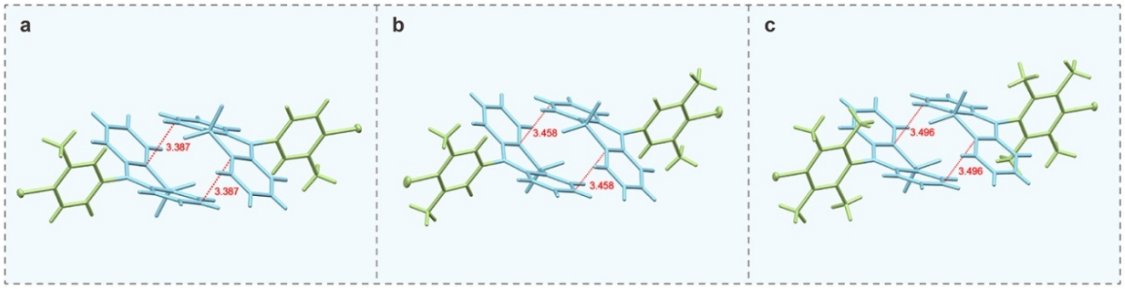

Fig. S12 Intermolecular interactions of adjacent dimer molecules in (a) **BrMOPP**, (b) **BrDMOPP**, and (c) **BrTMOPP** crystals.

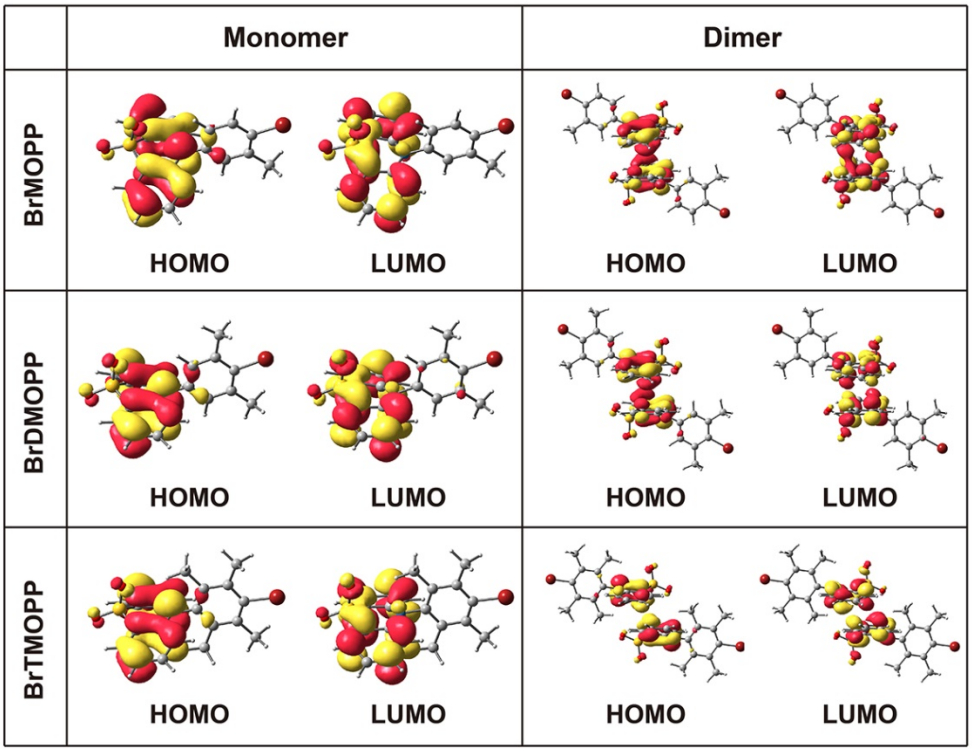

Fig. S13 Calculated the highest occupied molecular orbitals (HOMO) and the lowest unoccupied molecular orbitals (LUMO) of **BrMOPP**, **BrDMOPP**, and **BrTMOPP** in monomer and dimer.

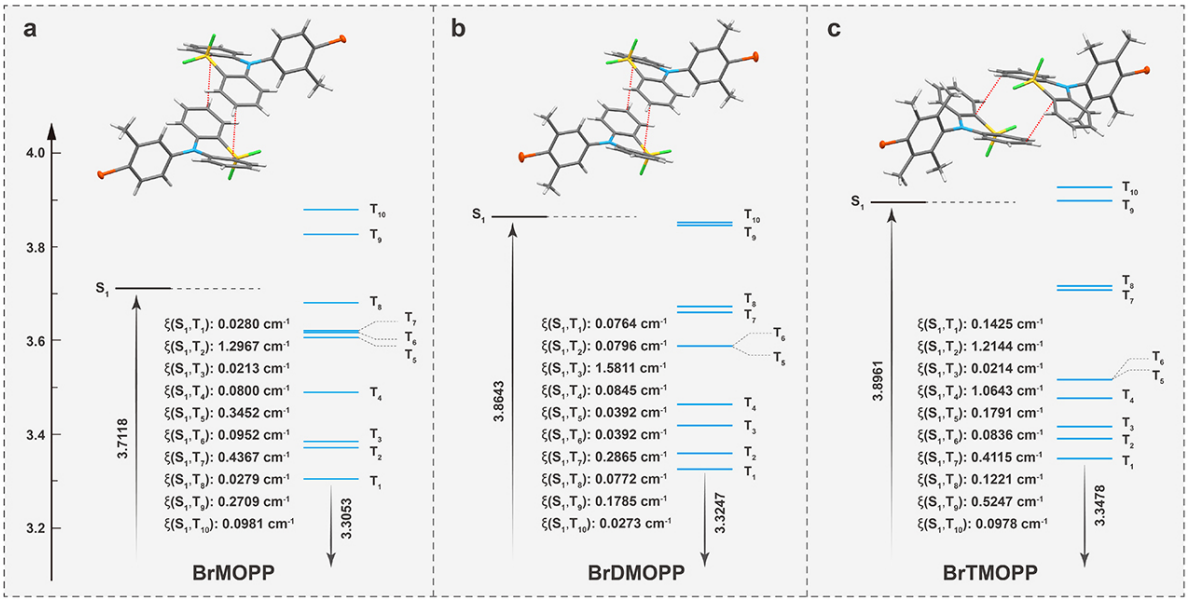

Fig. S14 Calculated energy diagram and spin-orbit coupling constant (ξ) of (a) **BrMOPP** dimer, (b) **BrDMOPP** dimer, and (c) **BrTMOPP** dimer in crystal states.

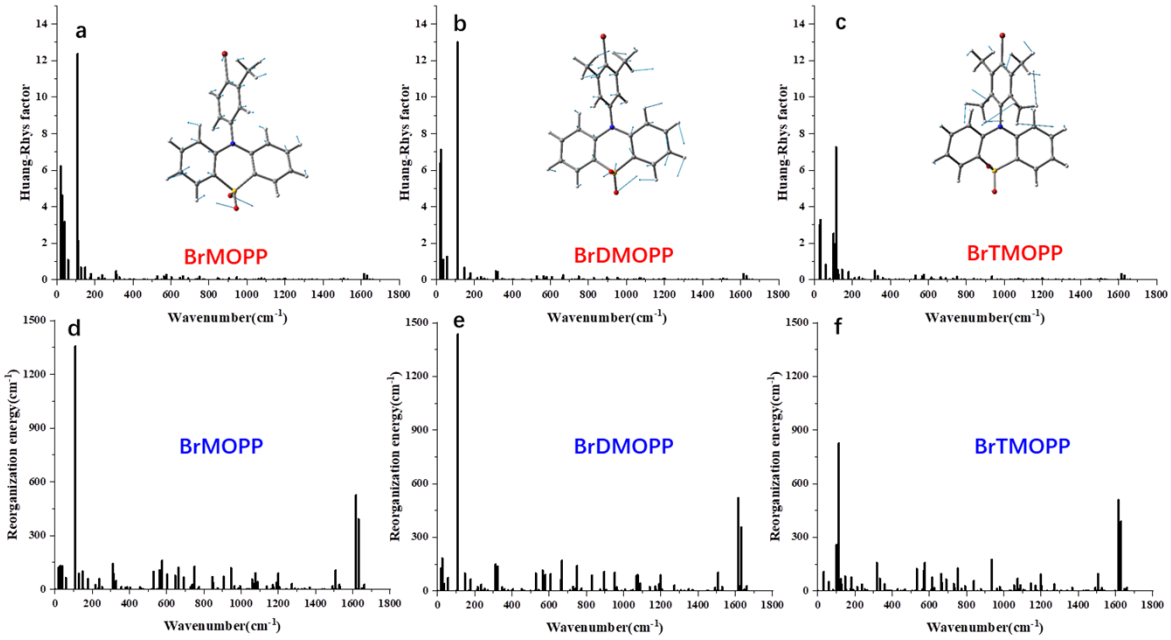

Fig. S15 The calculated Huang-Rhys factors, the displacement vectors of vibrational modes with the largest values of Huang-Rhys factors, and reorganization energies for **BrMOPP**, **BrDMOPP**, and **BrTMOPP** in crystals at T_1 states.

References

1 M. J. Frisch, G. W. Trucks, H. B. Schlegel, G. E. Scuseria, M. A. Robb, J. R. Cheeseman, G. Scalmani, V. Barone, B. Mennucci, G. A. Petersson, H. Nakatsuji, M. Caricato, X. Li, H. P. Hratchian, A. F. Izmaylov, J. Bloino, G. Zheng, J. L. Sonnenberg, M. Hada, M. Ehara, K. Toyota, R. Fukuda, J. Hasegawa, M. Ishida, T. Nakajima, Y. Honda, O. Kitao, H. Nakai, T. Vreven, J. A. Montgomery Jr., J. E. Peralta, F. Ogliaro, M. J. Bearpark, J. Heyd, E. N. Brothers, K. N. Kudin, V. N. Staroverov, R. Kobayashi, J. Normand, K. Raghavachari, A. P. Rendell, J. C. Burant, S. S. Iyengar, J. Tomasi, M. Cossi, N. Rega, N. J. Millam, M. Klene, J. E. Knox, J. B. Cross, V. Bakken, C. Adamo, J. Jaramillo, R. Gomperts, R. E. Stratmann, O. Yazyev, A. J. Austin, R. Cammi, C. Pomelli, J. W. Ochterski, R. L. Martin, K. Morokuma, V. G. Zakrzewski, G. A. Voth, P. Salvador, J. J. Dannenberg, S. Dapprich, A. D. Daniels, Farkas, J. B. Foresman, J. V. Ortiz, J. Cioslowski,

D. J. Fox, Gaussian 16, Revision B.01, Gaussian Inc., Wallingford CT, 2016.

2 ADF, SCM, Theoretical Chemistry, Virje Universiteit, Amsterdam, The Netherlands, 2016.

3 Y. Niu, W. Li, Q. Peng, H. Geng, Y. Yi, L. Wang, G. Nan, D. Wang and Z. Shuai, *Mol. Phys*., 2018, **116**, 1078-1090.

4 M. E. Casida, C. Jamorski, K. C. Casida and D. R. Salahub, *J. Chem. Phys.,* 1998, **108**, 4439-4449.

5 M. C. Li, M. Hayashi and S. H. Lin, *J. Phys. Chem. A,* 2011, **115**, 14531-14538.

6 Y. C. Duan, Y. Wu, J. L. Jin, D. M. Gu, Y. Geng, M. Zhang and Z. M. Su, *Chem. Phys. Chem.,* 2017, **18**, 755-762.

7 E. V. Lenthe, J. G. Snijders and E. J. Baerends, *J. Chem. Phys.,* 1996, **105**, 6505-6516.